Suppression of Cavity Time-Delay Signature Using Noise-Phase-Modulated Feedback

Han, Hong; Cheng, Xu Min; Jia, Zhi Wei; Shore, K. Alan

IEEE ACCESS

DOI:
10.1109/ACCESS.2020.2975359

Published: 28/02/2020

Publisher's PDF, also known as Version of record

Dyfyniad o'r fersiwn a gyhoeddwyd / Citation for published version (APA):
Han, H., Cheng, X. M., Jia, Z. W., & Shore, K. A. (2020). Suppression of Cavity Time-Delay Signature Using Noise-Phase-Modulated Feedback. *IEEE ACCESS*, *8*, 35344-35349. https://doi.org/10.1109/ACCESS.2020.2975359

IEEE Access
Multidisciplinary ⋮ Rapid Review ⋮ Open Access Journal

Received January 29, 2020, accepted February 16, 2020, date of publication February 20, 2020, date of current version February 28, 2020.

Digital Object Identifier 10.1109/ACCESS.2020.2975359

Suppression of Cavity Time-Delay Signature Using Noise-Phase-Modulated Feedback

HONG HAN[1,2], XU MIN CHENG[1], ZHI WEI JIA[1], AND K. ALAN SHORE[2], (Life Senior Member, IEEE)
[1]Key Laboratory of Advanced Transducers and Intelligent Control System, Ministry of Education, College of Physics and Optoelectronics, Taiyuan University of Technology, Taiyuan 030024, China
[2]School of Electronic Engineering, Bangor University, Wales LL57 1UT, U.K.

Corresponding author: Hong Han (hanhong@tyut.edu.cn)

This work was supported in part by the National Natural Science Foundation of China under Grant 61741512, Grant 61705160, Grant 61601319, Grant 61805168, Grant 61805170, and Grant 61805171, in part by the China Scholarship Council under Grant 201706935037, in part by the Natural Science Foundation of Shanxi Province under Grant 201801D221183, and in part by the Shanxi 1331 Project Key Innovative Research Team.

ABSTRACT We propose reconfiguration of the conventional feedback scheme to suppress the external-cavity time-delay signature (TDS) by adding noise phase modulation in the feedback of semiconductor laser. Noise-phase-modulated feedback introduces broad band noise frequencies into the feedback light and enables the suppression of the TDS. In this work, by means of simulations, the effect on TDS suppression of phase modulation (PM) index is explored. In addition, the influence of noise bandwidth variation is investigated. Using the auto-correlation function to quantity the TDS, we find that, for a large range of operating parameters, the TDS is significantly suppressed to the noise level and even submerged into the base noise. It is shown that suppression TDS is achievable over a wide operating parameter provided the noise generator bandwidth is of order 10 GHz and the PM index is greater than about 3. The proposed configuration will have widespread applications in contexts where suppression of the TDS is required.

INDEX TERMS Chaos, noise phase modulation, time-delay signature.

I. INTRODUCTION

Optical chaos has many potential applications in chaos-based secure communication [1], chaos key distribution [2], Brillouin optical correlation domain analysis [3], physical random number generation [4], optical reflectometry [5], and chaos radar [6]. An external-cavity semiconductor laser is a common method to generate optical chaos, but this approach can induce a time-delay signature (TDS) corresponding to the length of the external-cavity. Such a TDS can easily be extracted from the auto-correlation function (ACF) of a chaotic time series and also can be obtained from the RF spectrum of the chaos. Based on the correlation function, chaos can be used in optical time domain reflectometry for fault location in optical fibers [7]. However, in other applications of chaos such as, secure communication, key distribution, radar and random number generation, the presence of a TDS is not desirable. This is because the TDS induces periodic features into the dynamics which threaten the security of chaos communication [8], limit the key space [9], weaken anti-jamming capabilities [10] and reduce the randomness of bit sequences [11].

As means to suppress or even eliminate TDS, much work has been done in respect of the configuration of the optical feedback, including double feedback [12], FBG feedback [13], [14], chirped FBG feedback [15], random feedback [16], phased-array feedback [17], as well as phase-modulated feedback [18], [19]. With phase-modulated feedback, the bandwidth of chaos can be enhanced which is desirable in realizing high-speed communication.

Some driving signals of phase modulator based on self-delay or chaos in phase-modulated feedback have been proposed in recent research on chaos communications. Lavrov *et al.* reported delayed electo-optic phase modulation feedback and realized 10Gb/s transmission of a message hidden in chaos [20]. Jiang *et al.* used common chaotic phase-modulated optical feedback as an external-cavity structure to improve the communications performance [21].

The associate editor coordinating the review of this manuscript and approving it for publication was Chao-Yang Chen.

More recently, he proposed a physical WDM transmission by using chaotic spectral phase encryption where the phase modulator was driven by chaos from a chaos optical injection and a mirror feedback [22]. It was shown that the security of transmission arises partly from the complication of the driving signal of phase modulator, since any small difference from the authorized scheme prevents unauthorized attacks from decrypting the transmitted messages [22]. Also, the weak correlation between driving chaos synchronization signals and transmission carriers can improve the security performance in chaos communication, since such weaker correlation inhibits eavesdroppers illegal attacks from replicating the scheme of communication [21].

In this paper, we propose using noise as the driving signal of the phase modulator to achieve the suppression of the TDS. In comparison with the above mentioned driving signals of phase modulator, noise is a naturally stochastic signal, which has no correlation with the generated chaos in the system. Therefore, if noise-phase-modulated feedback were used in chaotic communication, it would require an enormous effort on the part of an unauthorized user to decrypt the transmitted messages, so the security will be further enhanced. One knows that the bandwidth of any photonic device is limited, so the bandwidth of noise generator containing an amplified spontaneous emission source, a photodetector and an electronic amplifier is considered in the simulation. The effects on the TDS of the bandwidth of noise generator are revealed. This bandwidth determines the phase modulation frequency.

The paper is structured as follows. A theoretical model of noise-phase-modulated feedback semiconductor laser is introduced in Section II. Mechanism for adding noise phase modulation is presented in Section III. The results given in Section IV delineate both phase modulation index and bandwidth of noise generator, that is phase modulation frequency, effects on suppression of the TDS. Finally, in section V, conclusions are drawn based on the results obtained.

II. THEORETICAL MODEL

The configuration of noise-phase-modulated feedback of semiconductor laser is illustrated in Fig.1. A phase modulator is deployed in the feedback of distributed feedback laser (DFB laser). The driving signals of phase modulator are from the noise generator which is comprised of an ASE source, a photodetector and an electronic amplifier.

Numerical simulations are based on the Lang-Kobayashi equations [23]. By adding the feedback term, the modified Lang-Kobayashi equations for the noise-phase-modulated feedback single-model semiconductor laser can be written as

$$\frac{dE(t)}{dt}=\frac{1}{2}(1+i\alpha)\left[\frac{g(N(t)-N_0)}{1+s|E(t)|^2}-\frac{1}{\tau_p}\right]E(t)+\sqrt{2\beta N(t)}\chi(t) + k_f E\left(t-\tau_f\right)\exp\left(-i\omega\tau_f\right)\exp\left(i\phi_{PM}(t)\right) \quad (1)$$

$$\frac{dN(t)}{dt}=\frac{I}{e}-\frac{N(t)}{\tau_e}-\frac{g(N(t)-N_0)}{1+s|E(t)|^2}|E(t)|^2 \quad (2)$$

$$\phi_{PM}(t)=\pi\beta_{PM}\chi_{PM}(t) \quad (3)$$

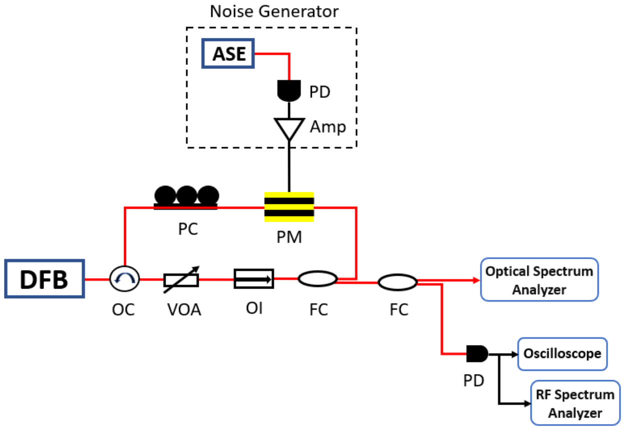

FIGURE 1. Schematic of noise phase modulated feedback of DFB laser. OC: optical coupler, PC: polarization controller, PM: phase modulator, ASE: amplified spontaneous emission, PD: photodetector, Amp: electronic amplifier, VOA: variable optical attenuator, OI: optical isolator, FC: fiber coupler.

$E(t)$ denotes the slow-varying complex electric field, and $N(t)$ denotes the carrier number in the laser cavity. The additional phase from the PM is presented in Eq. (3), where $\chi_{PM}(t)$ denotes the Gaussian noise (which is added at the phase modulator), which has zero mean and an amplitude ranging from -1 to 1. β_{PM} is the phase modulation index which is $\beta_{PM}=A/V_\pi$, where A is the amplitude of driving signal, and V_π is the half-wave voltage of phase modulator.

As a common method of quantifying the time-delay-signature, the auto-correlation function (ACF) is calculated. The ACF measures how well the time series matches its time-shifted replica, which is defined as [18], [21]

$$A(\Delta t)=\frac{\langle(I(t+\Delta t)-\langle I(t+\Delta t)\rangle)\cdot(I(t)-\langle I(t)\rangle)\rangle}{\sqrt{\left\langle(I(t+\Delta t)-\langle I(t+\Delta t)\rangle)^2\right\rangle\cdot\left\langle(I(t)-\langle I(t)\rangle)^2\right\rangle}} \quad (4)$$

where $I(t)=|E(t)|^2$ is the intensity time series, $I(t+\Delta t)$ contains the time shift Δt with respect to $I(t)$, and $\langle\cdot\rangle$ stands for the time averaging. The integration step used in the simulations is $dt=1$ ps. The definition and value of parameters in simulation are listed in Table 1, which are mainly ref. [21].

Considering the bandwidth of the photodetector and electronic amplifier, that is bandwidth of noise source generator, in the simulations we set the Gaussian noise $\chi_{PM}(t)$ through a low pass filter, which is used to control the bandwidth of the noise signal. Also in practice, the response modulation frequency of the phase modulator affects the output chaos. Here the response modulation frequency of the phase modulator is supposed 100 GHz, the maximum bandwidth of the noise source generator is no larger than 100 GHz. Therefore, only the bandwidth of the noise source generator, that is 3dB cut-off frequency of low pass filter, which also determines the modulation frequency, needs to be considered in simulation. In the simulations, the Gaussian noise $\chi_{PM}(t)$ has zero mean and variance from -1 to 1; when it passes the low pass filter, its amplitude will be reduced. In practice, the use of

TABLE 1. **Simulation parameter values [21].**

Parameter	Symbol	Value
Linewidth enhancement factor	α	5
Photon lifetime	τ_p	2 ps
Carrier lifetime	τ_e	2 ns
Threshold current	I_{th}	14.7 mA
Pump current	I	2 I_{th} or 5 I_{th}
Noise	$\chi(t)$	zero mean
Gain saturation coefficient	s	5.0×10^{-7}
Differential gain	g	1.5×10^{-8} ps^{-1}
Transparency inversion	N_0	1.5×10^{8}
Spontaneous emission rate	β	1.5×10^{-6} ns^{-1}
Feedback time	τ_f	5 ns
Feedback strength	k_f	20 ns^{-1} or 95 ns^{-1}

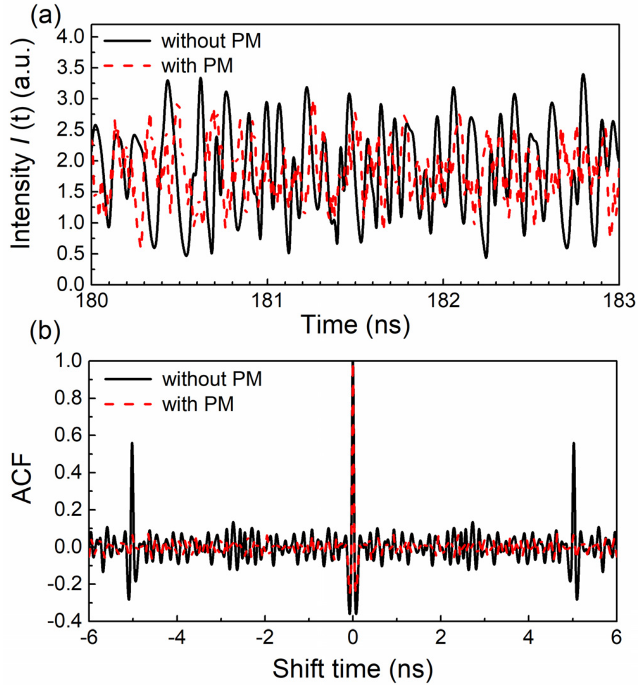

FIGURE 2. **Time series and ACF curves of chaos generated without PM(black) or with noise PM(red). The feedback strength and feedback time delay in both cases are respectively set as $k_f = 20$ ns^{-1}, $\tau_f = 5$ ns, and the pump current is $I = 2I_{th}$. The PM index is fixed as $\beta_{PM} = 4$, the bandwidth of noise generator (3dB low pass filter) is 40 GHz.**

an electronic amplifier, can enable amplification of the noise signals. Therefore, in order to demonstrate TDS suppression, the phase modulation index β_{PM} is set in the range 0 to 20.

III. MECHANISM

Here an outline is given of the underpinning physical effects which give rise to the advantageous use of noise-phase-modulated optical feedback in the suppression of the TDS. Since different frequencies are induced due to noise-phase-modulated feedback. Then as shown in Fig. 2(a), the temporal waveforms of the optical intensities display more fluctuation components as compared to the case of no PM. Here the PM index β_{PM} is 4 and the bandwidth of the noise generator is 40 GHz. When the feedback light contains many frequency components due to the noise PM, it is no longer a linear delayed replica of the output of the semiconductor laser. Therefore, as can be seen from the red curve of Fig. 2(b), with noise PM the TDS in ACF curve is significantly weakened.

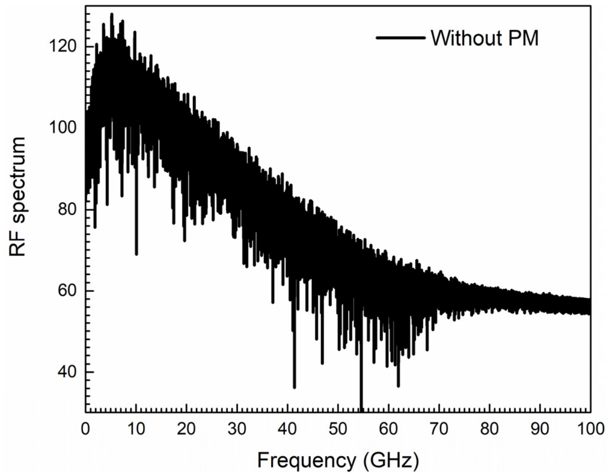

FIGURE 3. **RF spectrum of external-cavity optical feedback laser without phase-modulated. The feedback strength, feedback time delay and pump current are same as these in Fig.2, which are respectively set as $k_f = 20$ ns^{-1}, $\tau_f = 5$ ns, and $I = 2I_{th}$.**

To illustrate the mechanism of suppression TDS by noise-phase-modulated feedback, in this section the comparison cases without PM and with noise PM for different bandwidths of noise generator and varying modulation index are presented. For a typical external-cavity optical feedback semiconductor laser, the time-delay signature is clearly observed from the ACF as exemplified by the black curve in Fig. 2 (b) which comes from the linear delayed replica of the output chaos. Without PM, as shown in Figure 3, two dynamical effects are discernible from the RF spectrum. Firstly, relaxation oscillations produce periodical features near the peak of the RF spectrum. Secondly, the frequency difference between those features is determined by the external cavity round trip delay τ_f. It is found that the frequency difference between the features is 0.2 GHz which is $1/\tau_f$. After adding noise phase modulation feedback, as the PM index and noise generator bandwidth are increased both these dynamical features of chaos are highly weakened.

After adding noise-phase-modulated feedback, new frequency components are induced into the feedback light, and as a result, periodical peaks in RF spectrum are generally weakened, whilst high frequency components share the energy as Fig. 4(b1)-(b3) illustrate. It has also been observed here that the RF bandwidth of the output chaos using noise PM is enhanced with a remarkable enhancement being found at high bias current. From the ACF curves shown in Fig. 4(a1)-(a3), one can observe that the TDS gradually decreases as the bandwidth of the noise generator or the modulation index increases. Here, it is found that when the

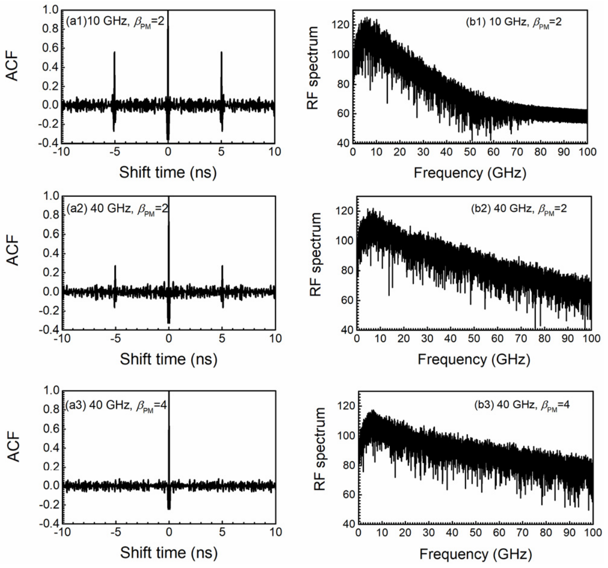

FIGURE 4. **ACF(a1-a3) and RF spectrum(b1-b3) of chaos using noise-phase-modulated feedback. The feedback strength, feedback time delay and bias current are same as these in case of Fig.2. (a1) and (b1): the noise generator bandwidth is 10 GHz, $\beta_{PM} = 2$; (a2) and (b2): the noise generator bandwidth is 40 GHz, $\beta_{PM} = 2$; (a3) and (b3): the noise generator bandwidth is 40 GHz, $\beta_{PM} = 4$.**

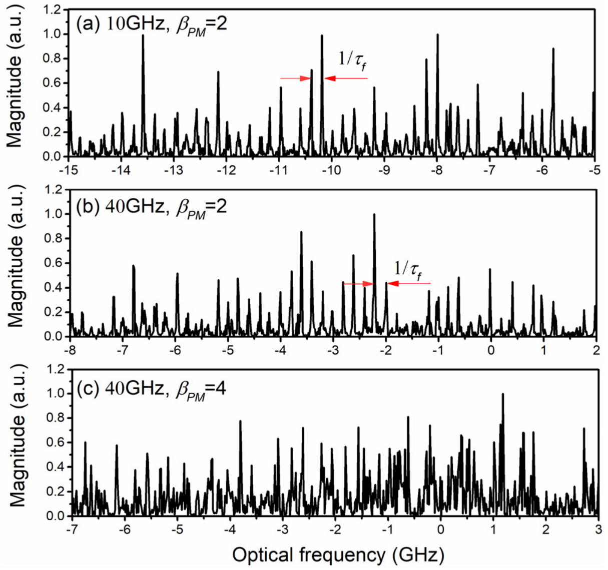

FIGURE 5. **Optical spectral of chaos using noise-phase-modulated feedback. All parameters values and conditions are same as these in Fig. 4.**

bandwidth of the noise generator reaches 40 GHz and the modulation index is 4, the periodical peaks in RF spectrum disappear as shown in Fig. 4(b3), whilst the TDS is totally suppressed as shown in Fig. 4(a3).

The above mentioned suppression process can be found from the optical spectral as shown in Fig. 5(a)-(c). When the bandwidth of the noise generator and the PM index are relatively small, the fixed mode spacing corresponding to the external-cavity ($1/\tau_f$) can be observed in the optical spectrum shown in Fig. 5(a). This feature is weakened as the bandwidth of the noise generator increases to 40 GHz (in Fig. 5(b)) and highly suppressed by further increasing the PM index to 4 (in Fig. 5(c)).

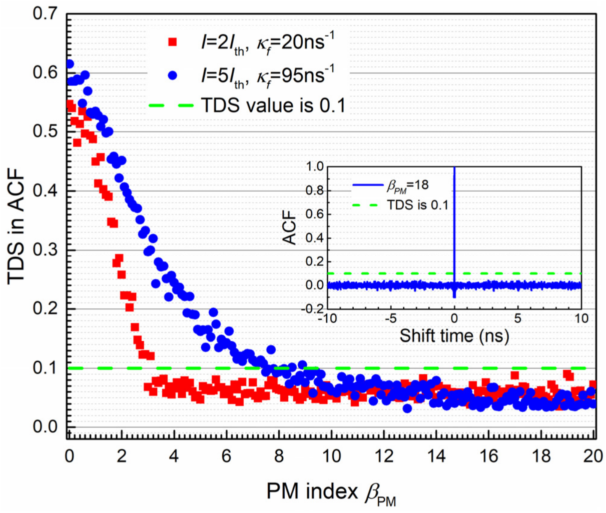

FIGURE 6. **TDS in ACF curve versus PM index. The bandwidth of noise generator (3dB low pass filter) is 40 GHz, and feedback time delay is 5 ns in both cases. Red squares denote $I = 2I_{th}$ under $k_f = 20$ ns^{-1}, blue circles denote $I = 5I_{th}$ under $k_f = 95$ ns^{-1}, green dashed line denotes 0.1 TDS value. Inset: ACF curve with conditions of $I = 5I_{th}$, $k_f = 95$ ns^{-1} and $\beta_{PM} = 18$.**

IV. SUPPRESSION RESULTS

Having established the main principles underpinning the approach taken here, attention is now given to detailed performance aspects.

A. PM INDEX EFFECTS

Attention is first given to the impact of the phase modulation index β_{PM} which is clearly a salient parameter of this process. Figure 6 shows results of the TDS in ACF versus PM index β_{PM}. It is found that as β_{PM} increases, the TDS in ACF decreasing quickly, then the TDS is suppressed to a relative small value. Even for the case of a relatively high laser bias current $I = 5I_{th}$, the TDS value can decrease from 0.62 to below 0.1(green dashed line) when the phase modulation index β_{PM} is above 8 as the blue circles shows in Fig. 6. If the index further increases to 18, the TDS will be submerged in the noise as the inset of Fig. 6 shows.

B. INFLUENCE OF THE NOISE GENERATOR BANDWIDTH

As well as the modulation index, the modulation frequency of the PM is an important factor which can be expected to affect the TDS suppression. As mentioned in Section II, we presume the modulation response frequency of PM is 100 GHz which is greater or equal to the bandwidth of the noise generator in use. Therefore, here consideration only needs to be given to the impact of the bandwidth of the noise generator, which finally determines the modulation frequency on PM. A low pass filter is used to control the bandwidth of the noise signal. By changing the 3dB bandwidth of low filter, the impact of the noise generator bandwidth can be

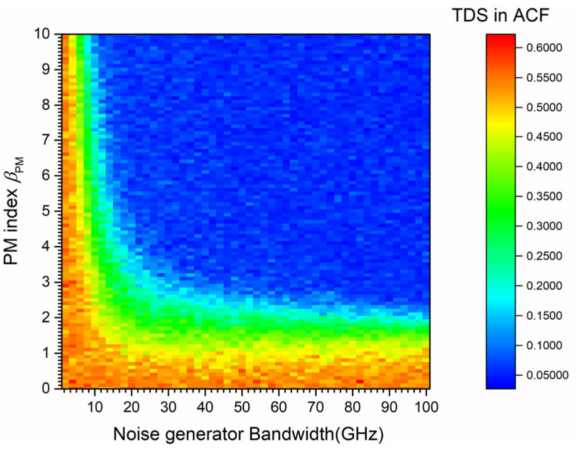

FIGURE 7. **TDS value in ACF curve versus PM index β_{PM} and bandwidth of the noise generator. Under conditions of $I = 2I_{th}$ and $k_f = 20$ ns^{-1}.**

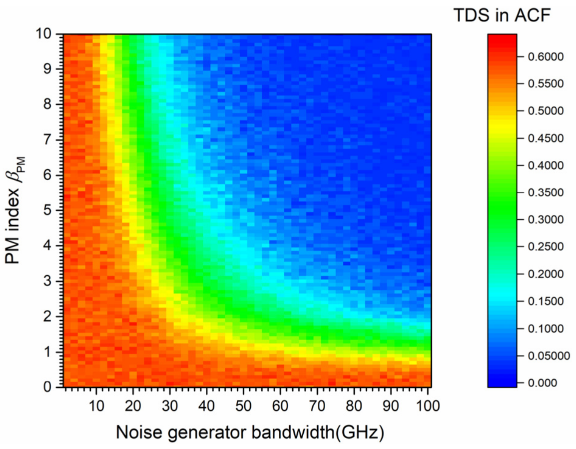

FIGURE 8. **TDS value in ACF curve versus PM index β_{PM} and bandwidth of the noise generator. Under conditions of $I = 5I_{th}$ and $k_f = 95$ ns^{-1}.**

determined, that is the effects of the modulation frequency on the TDS in the ACF.

Figures 7 and 8 show the variations of TDS value in ACF curve as a function of bandwidth of noise generator and PM index under relatively low pump current $2I_{th}$ and high pump current $5I_{th}$. As has been shown in detail in Figs. 4 and 5, the larger the noise generator bandwidth, higher frequencies can be induced into the phase term, thereby increasing the frequency components in the feedback light, and thus weakening the TDS. Based on this expectation, with increasing bandwidth of noise generator the TDS in the ACF generally decreases to a low level such as 0.1, which is the blue region in the right upper region of Figs. 7 and 8. The well suppressed TDS can be found in both conditions of relative weak feedback strength 20 ns^{-1} as shown in Fig. 7, and strong feedback strength of 95 ns^{-1} seen in Fig. 8. We also notice that if the bandwidth of noise generator is not sufficiently wide e.g. below 10 GHz in these both cases, the TDS remains around 0.2, even if the PM index is as high as 10. In any case, by comparing with the case of no PM, one can observe that the TDS value is well suppressed when the noise generator bandwidth is of order 10 GHz, whilst PM index should be larger than about 3 corresponding to the blue upper regions in Figs. 7 and 8.

V. CONCLUSION

A novel noise-phase-modulation feedback chaos laser has been proposed here. Noise as the driving signal of PM, induces a broad noise frequencies range into the feedback light and thus enable TDS suppression. This work has shown that over a large parameter range of PM index and noise generator bandwidth the TDS can be significant suppressed and even submerged into noise in a large parameter region. This study provides a new method to suppress TDS in a chaotic external cavity laser, which can be exploited in several application contexts.

REFERENCES

[1] A. Argyris, D. Syvridis, L. Larger, V. Annovazzi-Lodi, P. Colet, I. Fischer, J. García-Ojalvo, C. R. Mirasso, L. Pesquera, and K. A. Shore, “Chaos-based communications at high bit rates using commercial fibre-optic links,” *Nature*, vol. 438, no. 7066, pp. 343–346, Nov. 2005.

[2] Z. Zhao, M. Cheng, C. Luo, L. Deng, M. Zhang, S. Fu, M. Tang, P. Shum, and D. Liu, “Semiconductor-laser-based hybrid chaos source and its application in secure key distribution,” *Opt. Lett.*, vol. 44, no. 10, p. 2605, May 2019.

[3] J. Zhang, M. Zhang, M. Zhang, Y. Liu, C. Feng, Y. Wang, and Y. Wang, “Chaotic brillouin optical correlation-domain analysis,” *Opt. Lett.*, vol. 43, no. 8, p. 1722, Apr. 2018.

[4] L. Wang, D. Wang, H. Gao, Y. Guo, Y. Wang, Y. Hong, K. A. Shore, and A. Wang, “Real-time 2.5-Gb/s correlated random bit generation using synchronized chaos induced by a common laser with dispersive feedback,” *IEEE J. Quantum Electron.*, vol. 56, no. 1, pp. 1–8, Feb. 2020.

[5] Z. N. Wang, M. Q. Fan, L. Zhang, H. Wu, D. V. Churkin, Y. Li, X. Y. Qian, and Y. J. Rao, “Long-range and high-precision correlation optical time-domain reflectometry utilizing an all-fiber chaotic source,” *Opt. Express*, vol. 23, no. 12, pp. 15514–15520, Jun. 2015.

[6] M. Zhang, Y. Ji, Y. Zhang, Y. Wu, H. Xu, and W. Xu, “Remote radar based on chaos generation and radio over fiber,” *IEEE Photon. J.*, vol. 6, no. 5, pp. 1–12, Oct. 2014.

[7] T. Zhao, H. Han, J. Zhang, X. Liu, X. Chang, A. Wang, and Y. Wang, “Precise fault location in TDM-PON by utilizing chaotic laser subject to optical feedback,” *IEEE Photon. J.*, vol. 7, no. 6, pp. 1–9, Dec. 2015.

[8] M. Cheng, L. Deng, X. Gao, H. Li, M. Tang, S. Fu, P. Shum, and D. Liu, “Security-enhanced OFDM-PON using hybrid chaotic system,” *IEEE Photon. Technol. Lett.*, vol. 27, no. 3, pp. 326–329, Feb. 1, 2015.

[9] D. M. Wang, L. S. Wang, Y. Y. Guo, Y. C. Wang, and A. B. Wang, “Key space enhancement of optical chaos secure communication: Chirped FBG feedback semiconductor laser,” *Opt. Express*, vol. 27, no. 3, pp. 3065–3073, Jan. 2019.

[10] L. Wang, Y. Guo, P. Li, T. Zhao, Y. Wang, and A. Wang, “White-chaos radar with enhanced range resolution and anti-jamming capability,” *IEEE Photon. Technol. Lett.*, vol. 29, no. 20, pp. 1723–1726, Oct. 15, 2017.

[11] A. Wang, L. Wang, P. Li, and Y. Wang, “Minimal-post-processing 320-Gbps true random bit generation using physical white chaos,” *Opt. Express*, vol. 25, no. 4, pp. 3153–3164, Feb. 2017.

[12] J.-G. Wu, G.-Q. Xia, and Z.-M. Wu, “Suppression of time delay signatures of chaotic output in a semiconductor laser with double optical feedback,” *Opt. Express*, vol. 17, no. 22, Oct. 2009, 20124.

[13] Z.-Q. Zhong, Z.-M. Wu, and G.-Q. Xia, “Experimental investigation on the time-delay signature of chaotic output from a 1550 nm VCSEL subject to FBG feedback,” *Photon. Res.*, vol. 5, no. 1, pp. 6–10, Dec. 2016.

[14] S.-S. Li, Q. Liu, and S.-C. Chan, “Distributed feedbacks for time-delay signature suppression of chaos generated from a semiconductor laser,” *IEEE Photon. J.*, vol. 4, no. 5, pp. 1930–1935, Oct. 2012.

[15] D. Wang, L. Wang, T. Zhao, H. Gao, Y. Wang, X. Chen, and A. Wang, “Time delay signature elimination of chaos in a semiconductor laser by dispersive feedback from a chirped FBG,” *Opt. Express*, vol. 25, no. 10, pp. 10911–10924, May 2017.

[16] Y. Xu, M. Zhang, L. Zhang, P. Lu, S. Mihailov, and X. Bao, “Time-delay signature suppression in a chaotic semiconductor laser by fiber random grating induced random distributed feedback,” *Opt. Lett.*, vol. 42, no. 20, p. 4107, Oct. 2017.

[17] P. Zhou, Q. Fang, and N. Li, "Phased-array assisted time-delay signature suppression in the optical chaos generated by an external-cavity semiconductor laser," *Opt. Lett.*, vol. 45, no. 2, p. 399, Jan. 2020.
[18] S. Xiang, W. Pan, L. Zhang, A. Wen, L. Shang, H. Zhang, and L. Lin, "Phase-modulated dual-path feedback for time delay signature suppression from intensity and phase chaos in semiconductor laser," *Opt. Commun.*, vol. 324, pp. 38–46, Aug. 2014.
[19] N. Jiang, A. Zhao, S. Liu, C. Xue, B. Wang, and K. Qiu, "Generation of broadband chaos with perfect time delay signature suppression by using self-phase-modulated feedback and a microsphere resonator," *Opt. Lett.*, vol. 43, no. 21, p. 5359, Oct. 2018.
[20] R. Lavrov, M. Jacquot, and L. Larger, "Nonlocal nonlinear electro-optic phase dynamics demonstrating 10 Gb/s chaos communications," *IEEE J. Quantum Electron.*, vol. 46, no. 10, pp. 1430–1435, Oct. 2010.
[21] N. Jiang, A. Zhao, S. Liu, C. Xue, and K. Qiu, "Chaos synchronization and communication in closed-loop semiconductor lasers subject to common chaotic phase-modulated feedback," *Opt. Express*, vol. 26, no. 25, pp. 32404–32416, Dec. 2018.
[22] N. Jiang, A. Zhao, C. Xue, J. Tang, and K. Qiu, "Physical secure optical communication based on private chaotic spectral phase encryption/decryption," *Opt. Lett.*, vol. 44, no. 7, pp. 1536–1539, Mar. 2019.
[23] R. Lang and K. Kobayashi, "External optical feedback effects on semiconductor injection laser properties," *IEEE J. Quantum Electron.*, vol. 16, no. 3, pp. 347–355, Mar. 1980.

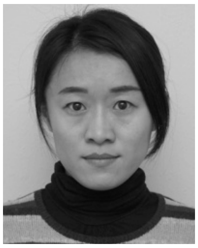

HONG HAN received the B.S. degree in physics from the University of Jiamusi, Jiamusi, China, in 2007, and the Ph.D. degree from the Harbin Institute of Technology, Harbin, China, in 2014.

She was a Lecturer with the Taiyuan University of Technology from 2014 to 2017 and then she became an Associate Professor in 2017. She is currently a Postdoctoral Researcher with Bangor University. Her research work is in dynamic features of chaotic lasers and chaotic security communication. She is a member of OSA.

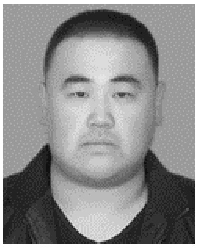

XU MIN CHENG received the B.S. degree in electronic information science and technology from the University of Changzhi, Changzhi, China, in 2019. He is currently pursuing the degree with the Taiyuan University of Technology. His research work is in dynamic features of chaotic lasers.

ZHI WEI JIA received the Ph.D. degree from the Institute of Semiconductors, Chinese Academy of Sciences, in 2017. Since September 2017, he has been working as a Lecturer with the Taiyuan University of Technology. His research interests include the single-mode quantum cascade lasers and their applications such as trace gas detection and laser spectroscopy.

K. ALAN SHORE (Life Senior Member, IEEE) received the degree in mathematics from the University of Oxford, Oxford, U.K., and the Ph.D. degree from University College, Cardiff, Wales, U.K. He was a Lecturer with the University of Liverpool, from 1979 to 1983, and then at the University of Bath where he became a Senior Lecturer in 1986, a Reader in 1990, and a Professor in 1995. He was a Visiting Researcher with the Center for High Technology Materials, University of New Mexico, Albuquerque, USA, in 1987. In 1989, he was a Visiting Researcher with the Huygens Laboratory, Leiden University, The Netherlands. From summer 1990 to 1991, he was with the Teledanmark Research Laboratory, Technical University of Denmark, Lyngby, and also with the MIDIT Center, Technical University of Denmark. He was a Guest Researcher with the Electrotechnical Laboratory, Tsukuba, Japan, in 1991. In 1992, he was a Visiting Professor with the Department of Physics, University de les Illes Balears, Palma-Mallorca, Spain. He was a Visiting Lecturer with the Instituto de Fisica de Cantabria, Santander, Spain, in June 1996 and 1998, and also a Visiting Researcher with the Department of Physics, Macquarie University, Sydney, Australia, in 1996, 1998, 2000, 2002, 2005, and 2008. From July to August 2001, he was a Visiting Researcher with ATR Adaptive Communications Laboratories, Kyoto, Japan. In 1995, he was appointed to the Chair of electronic engineering with Bangor University, where he has been the Head of the School of Informatics and of the College of Physical and Applied Sciences. From 2001 to 2008, he was the Director of industrial and commercial optoelectronics a Welsh Development Agency Centre of Excellence. He has chaired the Photonics Academy for Wales, since its establishment in 2005. He was the Chair of the Welsh Optoelectronics Forum from 2006 to 2008. From 2008 to 2011, he was the Chair of the Quantum Electronics Commission, International Union of Pure and Applied Physics. In 2015, he coordinated activities in Wales related to the International Year of Light. In 2017, he chaired the Science and Technology Committee of the National Eisteddfod of Wales. He has authored or coauthored more than 1000 contributions to archival journals, books, and technical conferences. With Prof. D. Kane, he co-edited the research monograph Unlocking Dynamical Diversity. His current research interests include the dynamics of vertical-cavity semiconductor lasers, applications of nonlinear dynamics in semiconductor lasers, and the design of nano-spin semiconductor lasers. His research work has been principally in the area of semiconductor optoelectronic device design and experimental characterization with particular emphasis on nonlinearities in laser diodes and semiconductor optical waveguides.

Prof. Shore has been a Program Member of several OSA conferences and was a Co-organizer of a Rank Prize Symposium on Nonlinear Dynamics in Lasers held at Lake, U.K., in August 2002. He is a Fellow of the Optical Society of America, the Institute of Physics, and the Learned Society of Wales for which he has served as a Council Member from 2012 to 2015 and from 2016 to 2019 and a General Secretary from 2017 to 2020. He received a Royal Society Travel Grant to visit universities and laboratories in Japan in July 1988. From July to December 2010, he held a Japan Society for the Promotion of Science Invitation Fellowship in the Ultrafast Photonics Group, Graduate School of Materials Science, Nara Institute of Science and Technology, Nara, Japan. He chaired the Education and Training in Optics and Photonics conference held at the Technium OpTIC, Wales, 2009. He cofounded and from 1987 to 2012 acted as the Organizer and a Program Committee Chair for the International Conference on Semiconductor and Integrated Optoelectronics, which is held annually in Cardiff, Wales, U.K.

• • •